Article

Transition State Structure of *E. coli t*RNA-Specific Adenosine Deaminase

Minkui Luo, and Vern L. Schramm

J. Am. Chem. Soc., **2008**, 130 (8), 2649-2655 • DOI: 10.1021/ja078008x

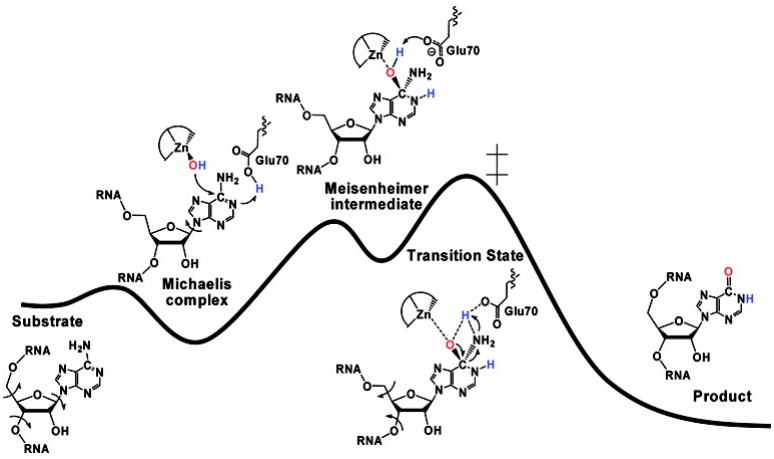

More About This Article

Additional resources and features associated with this article are available within the HTML version:

- Supporting Information
- Links to the 1 articles that cite this article, as of the time of this article download
- Access to high resolution figures
- Links to articles and content related to this article
- Copyright permission to reproduce figures and/or text from this article

View the Full Text HTML

J|A|C|S
ARTICLES
Published on Web 02/02/2008

Transition State Structure of *E. coli* *t*RNA-Specific Adenosine Deaminase

Minkui Luo and Vern L. Schramm*

Department of Biochemistry, Albert Einstein College of Medicine, Bronx, New York 10461

Received October 18, 2007; E-mail: vern@aecom.yu.edu.

Abstract: Bacterial *t*RNA-specific adenosine deaminase (TadA) catalyzes the essential deamination of adenosine to inosine at the wobble position of *t*RNAs and is necessary to permit a single *t*RNA species to recognize multiple codons. The transition state structure of *Escherichia coli* TadA was characterized by kinetic isotope effects (KIEs) and quantum chemical calculations. A stem loop of *E. coli* $tRNA^{Arg2}$ was used as a minimized TadA substrate, and its adenylate editing site was isotopically labeled as [1′-^{3}H], [5′-$^{3}H_2$], [1′-^{14}C], [6-^{13}C], [6-^{15}N], [6-^{13}C, 6-^{15}N] and [1-^{15}N]. The intrinsic KIEs of 1.014, 1.022, 0.994, 1.014 and 0.963 were obtained for [6-^{13}C]-, [6-^{15}N]-, [1-^{15}N]-, [1′-^{3}H]-, [5′-$^{3}H_2$]-labeled substrates, respectively. The suite of KIEs are consistent with a late S_NAr transition state with a complete, *pro-S*-face hydroxyl attack and nearly complete N1 protonation. A significant N6−C6 dissociation at the transition state of TadA is indicated by the large [6-^{15}N] KIE of 1.022 and corresponds to an N6−C6 distance of 2.0 Å in the transition state structure. Another remarkable feature of the *E. coli* TadA transition state structure is the Glu70-mediated, partial proton transfer from the hydroxyl nucleophile to the N6 leaving group. KIEs correspond to H−O and H−N distances of 2.02 and 1.60 Å, respectively. The large inverse [5′-^{3}H] KIE of −3.7% and modest normal [1′-^{3}H] KIE of 1.4% indicate that significant ribosyl 5′-reconfiguration and purine rotation occur on the path to the transition state. The late S_NAr transition-state established here for *E. coli* TadA is similar to the late transition state reported for cytidine deaminase. It differs from the early S_NAr transition states described recently for the adenosine deaminases from human, bovine, and *Plasmodium falciparum* sources. The *ec*TadA transition state structure reveals the detailed architecture for enzymatic catalysis. This approach should be readily transferable for transition state characterization of other RNA editing enzymes.

Introduction

Posttranscriptional RNA editing is the modification of RNA sequence that is distinct from RNA splicing, capping or 5′ end processing. Both *t*RNA-specific adenosine deaminase (TadA) and adenosine deaminase that acts on *ds*RNA (ADAR) operate on complex RNA substrates (Figure 1).[1−4] Posttranscriptional *t*RNA editing involves TadA-catalyzed adenosine to inosine conversion (A-to-I) at the wobble position.[5,6] The TadA activity is essential for a single *t*RNA species to recognize multiple codons since inosine is recognized as guanosine in base pairing.[3,4] ADARs carry out A-to-I conversion on *ds*RNA, and this editing is prevalent in mammals and occurs in up to 10% of all mRNAs containing inosine.[7] This editing event can alter the primary sequence codon, splice sites and structures of edited RNA because inosine is recognized as guanosine in most cellular processes. ADAR activities are necessary for neuron receptor diversification[8,9] and hepatitis delta virus replication.[10,11] For the latter, A-to-I editing switches an amber stop codon (U**A**G) to a tryptophan (U**I**G) for expressing fully functioned proteins.

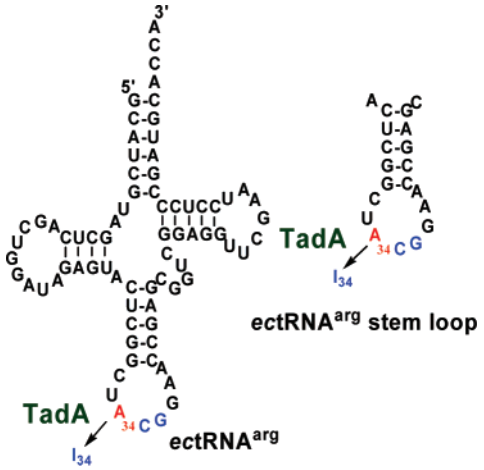

Figure 1. Structures of *ect*RNA^{arg2} and its truncated stem loop. The structure of full-length *ect*RNA^{arg2} is shown in the left. The anticodon region is highlighted with red and blue, and the TadA-editing site is red. The truncated *ect*RNA^{arg2} stem loop is shown to the right with the same scheme. *ec*TadA targets the A_{34} sites of these constructs with similar catalytic activity. Adenosine A_{34} is converted to inosine (I_{34}) by the deamination reaction.[3,5]

(1) Elias, Y.; Huang, R. H. *Biochemistry* **2005**, *44*, 12057−12065.
(2) Kuratani, M.; Ishii, R.; Bessho, Y.; Fukunaga, R.; Sengoku, T.; Shirouzu, M.; Sekine, S.; Yokoyama, S. *J. Biol. Chem.* **2005**, *280*, 16002−16008.
(3) Kim, J.; Malashkevich, V.; Roday, S.; Lisbin, M.; Schramm, V. L.; Almo, S. C. *Biochemistry* **2006**, *45*, 6407−6416.
(4) Losey, H. C.; Ruthenburg, A. J.; Verdine, G. L. *Nat. Struct. Mol. Biol.* **2006**, *13*, 153−159.
(5) Wolf, J.; Gerber, A. P.; Keller, W. *EMBO J.* **2002**, *21*, 3841−3851.
(6) Gerber, A. P.; Keller, W. *Science* **1999**, *286*, 1146−1149.
(7) Bass, B. L. *Annu. Rev. Biochem.* **2002**, *71*, 817−846.

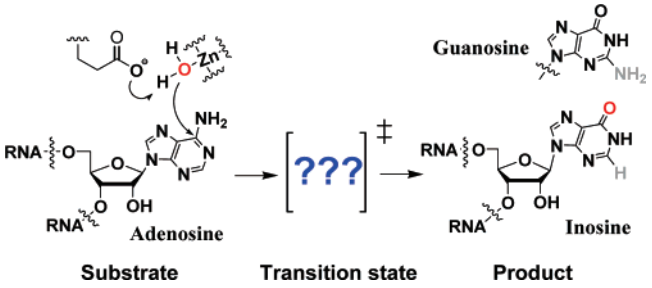

Figure 2. TadA-mediated adenosine deamination. The initial step proposed for TadA-catalyzed demination is formation of Zn^{2+}-hydroxyl. The nearby Glu residue serves as the general base to remove proton from Zn-bound water. The structures of guanosine and the product inosine are shown. Inosine in edited RNA is recognized as guanosine.

Recent studies on human ADAR substrates further led to identifying a new A-to-I editing target *BC10* that has been linked to bladder cancer and renal cancer proliferation. hADAR is also characterized as one of few unambiguously up-regulated genes in solid tumors and liver cancer.[12−14] These pieces of evidence strongly relate ADAR upregulation to cancer progression. ADARs also process microRNAs and therefore alter expression or target specificity of the microRNAs.[15,16] Our interest in transition-state structure led us to solve the transition state structure of TadA, an RNA editing enzyme which targets a structurally complex and biologically relevant *t*RNAs from *Escherichia coli* (Figures 1 and 2).

KIEs are one of the few tools to characterize enzyme transition states in structural detail.[17−20] The elucidation of enzyme transition state structure is valuable in the development of potent inhibitors. Molecules that mimic enzymatic transition states are expected to show K_d values of 10^{-18}−10^{-21} M, proportional to the enzyme-imposed rate enhancement of catalysis.[21] We have applied this approach to achieve inhibitors with pM to fM affinities for *N*-ribosyltransferase enzymes.[21] Here we apply similar approaches to probe the more complex transition state structure of TadA. The results are of potential utility for the design of transition state analogue inhibitors in the family of RNA editing enzymes.

Kinetic isotope effects are reported for the deamination of RNA by *E. coli* TadA using substrates whose editing sites were labeled with [6-^{13}C], [6-^{15}N], [1-^{15}N], [5′-$^{3}H_2$], and [1′-^{3}H]. The transition state structure of *ec*TadA was explored with KIE-constrained quantum chemical calculations. Intrinsic KIEs of

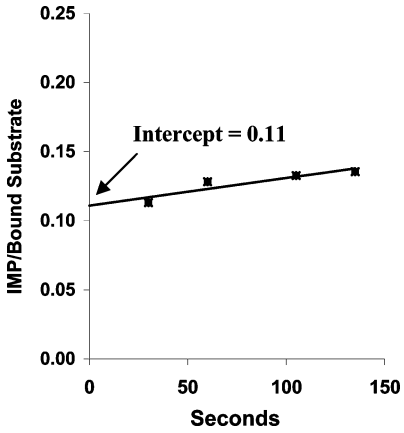

Figure 3. Measurement of forward commitment factor of *ec*TadA.[18,19] The isotope trapping experiment for measuring the forward commitment was performed under rapid-mixing pre-steady-state conditions. Enzyme was bound to the labeled substrate in a 2 ms mix and was then diluted into a large excess of unlabeled cold substrate. The ratio of IMP formed to enzyme-bound substrate was plotted vs time. The forward commitment factor (C_f) was calculated from the ordinate intercept, fit to a linear equation with C_f = 0.15.

1.014, 1.022, and 0.993 were obtained for primary [6-^{13}C]-, [6-^{15}N], and secondary [1-^{15}N] positions, respectively. This suite of KIEs was used as constraints to model a transition state for *ec*TadA. *ec*TadA adopts a late S_NAr transition state with a complete, *pro-S*-face hydroxyl addition, nearly complete N1 protonation and significant N6−C6 dissociation. The rate-limiting step of the *ec*TadA-catalyzed deamination is subsequent to the formation of the tetrahedral Meisenheimer intermediate. Computational analysis of the reaction supports a transition state with a proton shuttle between the hydroxyl nucleophile and the leaving group N6, mediated by nearby Glu70. Significant distortion of the 5′-sugar and rotation of the ribosidic purine on the path to transition state formation were indicated from the large inverse [5′-$^{3}H_2$] KIE of −4% and significant [1′-^{3}H] KIE of 1.4%. This is the first time that KIEs have been correlated with purine base rotation at an RNA-based transition state. We propose that this KIE approach will be useful for transition state and base rotation characterization of other RNA editing enzymes. The *ec*TadA transition state structure reveals the detailed architecture for catalytic efficiency and provides a blueprint for designing tight-binding inhibitors.

Experimental Section

Expression and Purification of *ec*TadA. A 13aa-truncated *ec*TadA was expressed and purified as described previously with some modification.[3] Here the *ec*TadA was subject to two additional MonoQ columns (GE Science) and a Superdex75 purification (GE Science) to lower RNase activities.

Synthesis of Isotopically Labeled Substrates. [1′-^{3}H]-, [5′-$^{3}H_2$]-, [1′-^{14}C]-, [1′-^{14}C, 6-^{13}C], [1′-^{14}C, 6-^{15}N], [1′-^{14}C, 6-^{13}C^{15}N], and [1′-^{14}C, 1-^{15}N]-labeled ATPs were prepared enzymatically as described previously.[18,19] The isotopically labeled stem loops were synthesized by incorporating labeled ATPs via the T7 RNA polymerase reaction (MEGAshort script T7 kit, Ambion). See Supporting Information for detailed information.

Measurement of Commitment Factor. Forward commitment for *ec*TadA-catalyzed deamination was determined by an isotope trapping method under rapid-mixing presteady-state conditions (Figure 3).[18,19] Briefly, 25.1 μL of 30 μM *ec*TadA stock was rapidly mixed with 20.9 μL of 36.5 μM [1′-^{3}H]-labeled *ec*tRNA^{arg2} stem loop substrate (total 2 × 10^5 cpm) for 2 ms using a quench flow apparatus (PQF-3, KinTek).

(8) Macbeth, M. R.; Schubert, H. L.; VanDemark, A. P.; Lingam, A. T.; Hill, C. P.; Bass, B. L. *Science* **2005**, *309*, 1534−1539.
(9) Tonkin, L. A.; Saccomanno, L.; Morse, D. P.; Brodigan, T.; Krause, M.; Bass, B. L. *EMBO J.* **2002**, *21*, 6025−6035.
(10) Wong, S. K.; Lazinski, D. W. *Proc. Natl. Acad. Sci. U.S.A.* **2002**, *99*, 15118−15123.
(11) Sato, S.; Wong, S. K.; Lazinski, D. W. *J. Virol.* **2001**, *75*, 8547.
(12) Pilarsky, C.; Wenzig, M.; Specht, T.; Saeger, H. D.; Grutzmann, R. *Neoplasia* **2004**, *6*, 744−750.
(13) Midorikawa, Y.; Tsutsumi, S.; Taniguchi, H.; Ishii, M.; Kobune, Y.; Kodama, T.; Makuuchi, M.; Aburatani, H. *Jpn. J. Cancer Res.* **2002**, *93*, 636−643.
(14) (a) Clutterbuck, D. R.; Leroy, A.; O'Connell, M. A.; Semple, C. A. *Bioinformatics* **2005**, *21*, 2590−2595. (b) Gromova, I.; Gromov, P.; Celis, J. E. *Int. J. Cancer* **2002**, *98*, 539−546.
(15) Kawahara, Y.; Zinshteyn, B.; Sethupathy, P.; Iizasa, H.; Hatzigeorgiou, A. G.; Nishikura, K. *Science* **2007**, *315*, 1137−1140.
(16) Yang, W. D.; Chendrimada, T. P.; Wang, Q. D.; Higuchi, M.; Seeburg, P. H.; Shiekhattar, R.; Nishikura, K. *Nat. Struct. Mol. Biol.* **2006**, *13*, 13−21.
(17) Cleland, W. W. *Arch. Biochem. Biophys.* **2005**, *433*, 2−12.
(18) Luo, M.; Singh, V.; Taylor, E. A.; Schramm, V. L. *J. Am. Chem. Soc.* **2007**, *129*, 8008−8017.
(19) Singh, V.; Schramm, V. L. *J. Am. Chem. Soc.* **2007**, *129*, 2783−2795.
(20) Schramm, V. L. *Curr. Opin. Struct. Biol.* **2005**, *15*, 604−613.
(21) Schramm, V. L. *Arch. Biochem. Biophys.* **2005**, *433*, 13−26.

The reaction mixture was then rapidly injected into a chase solution containing 40 μM unlabeled substrate to give the final volume of 1 mL. Subsequently, 100 μL aliquots were collected every 30 s for 2.5 min and quenched with 50 μL of 1 N HCl for 3 min, followed by neutralization with 50 μL of 1 N KOH. The subsequent chase solutions were subject to pH adjustment, P1 digestion, and HPLC purification (Supporting Information), to resolve IMP as the reaction products. The total cpm of IMP generated after the chase step was corrected for background counting, obtained from a control in the absence of enzyme, and the cpm of IMP generated during mixing, calculated on the basis of $k_{cat} = 13$ min^{-1}, the enzyme concentration and the mixing time.[3] The amount of enzyme-bound substrate prior to the chase step was calculated on the basis of $K_m = 0.83\ \mu$M[3] and the enzyme concentration. The ratios of [1′-^{3}H]IMP product to *ec*TadA-bound substrate were plotted vs time *t*. The forward commitment factor C_f was obtained from the ordinate intercept upon extrapolation to zero time (Figure 3, forward commitment= intercept/(1 − intercept)). The *ec*TadA-catalyzed deamination is irreversible and therefore its reverse commitment factor is zero. Consequently, eq 1 was used for commitment factor correction, in which $^X(V/K)$ is the observed heavy atom KIE, ^Xk is the intrinsic KIE, ^XK is the equilibrium isotope effect between substrate and product, C_f and C_r stand as the forward and reverse commitment, respectively. C_r is expected to be zero in this case.

$$^X(V/K) = \frac{^Xk + C_f + C_r \times {}^XK_{eq}}{1 + C_f + C_r} \quad (1)$$

KIE Determination. All *ec*TadA-catalyzed deamination reactions were carried out at 25 °C in a buffer containing 10 mM Tris-HCl, 10 mM KCl, 5% glycerol (v/v), 25 μM of the stem loop substrate (labeled and unlabeled), 100 unit/mL RNasin Plus RNase inhibitor (Promega), and 100 nM *ec*TadA. Apparent KIEs were determined by the competitive radiolabeled method (Supporting Information).[18,19]

Computational Modeling. With the intrinsic KIEs as constraints, the *ec*TadA transition state structure was determined *in vacuo* using hybrid density functional methods with B3LYP/6-31G (d,p) level of theory implemented in Gaussian 98 (Supporting Information). We used 9-methyladenine as a truncated substrate and a hydroxyl anion as the nucelophile for calculating the [6-^{13}C], [6-^{15}N], and [1-^{15}N] KIE values.[18] The transition state structures were optimized from a fully formed Meisenheimer intermediate by varying C6-O^{hydroxyl}, C6−N6 bond distances as well as the degree of O^{hydroxyl}, N1 and NH$_2$-6 protonation. Bond frequencies for the substrate and transition states were calculated and used as the inputs to the ISOEFF98 program for KIE determination.[22] The remote isotope effects were calculated using 3′-phosphate-5′-methylphosphate adenosine and its C6 hydroxyl adduct for the [5′-^{3}H$_2$] and [1′-^{3}H] KIE values. Their initial geometry (reactant) was extracted from the NMR structure reported for *ec*tRNA^{Phe} G$_{34}$ residue (PDB, 1KKA).[23] Structural candidates for the transition state were generated on the basis of TadA-bound RNA^{arg2} A$_{34}$ analogue (PDB, 2B3J).[4] with its purine base replaced with 6-hydroxyl adenine (9-methyladenine mimic of the transition state described above). Structural candidates were generated by imposing constraints or varying the dihedral angles that influence the [1′-^{3}H] and [5′-^{3}H$_2$] KIEs. The structures were optimized at the B3LYP/6-31G (d,p) level of theory. Bond vibrational frequencies and KIEs were calculated as described above. The structure of the TadA-bound Michaelis complex was modeled by releasing all constraints except the C8−N9−C1′−O4 dihedral angle of 73.5° based on the structure of the residue 34 of TadA-bound RNA^{arg2}.[4] The structure of the Meisenheimer intermediate was optimized by restricting the C8−N9−C1′−O4 dihedral angle to 45.0° and the N1−H distance to 1.10 Å.

(22) Anisimov, V.; Paneth, P. *J. Math. Chem.* **1999**, *26*, 75−86.
(23) Cabello-Villegas, J.; Winkler, M. E.; Nikonowicz, E. P. *J. Mol. Biol.* **2002**, *319*, 1015−1034.

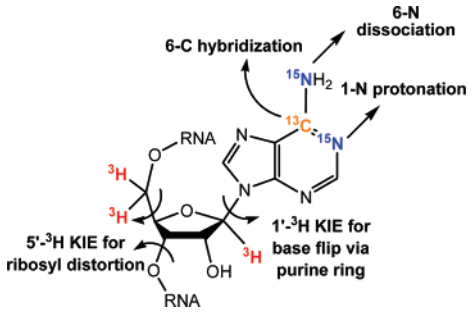

Figure 4. Isotopic reporters for transition state structure. The magnitude of the [6-^{13}C], [6-^{15}N], [1-^{15}N], [5′-^{3}H$_2$], and [1′-^{3}H] KIEs reflect the degree of C6 hybridization, N6 dissociation, N1 protonation, 5′-ribosyl distortion, and ribosidic purine ring rotation at the TadA transition state, respectively. Color codes for isotopic atoms: ^{13}C, yellow; ^{15}N, blue; ^{3}H, red.

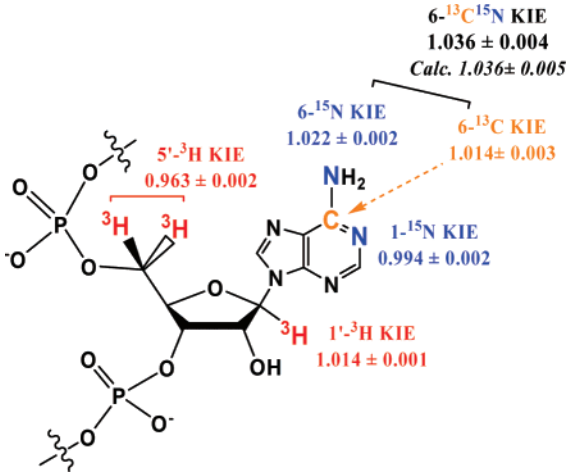

Figure 5. KIEs for TadA-catalyzed deamination. All reported KIEs are intrinsic following commitment factor correction. Details of the KIE and forward commitment factor measurements are provided in the Supporting Information. The calculated [6-^{13}C, ^{15}N] KIE is the product of [6-^{13}C] and [6-^{15}N] KIEs and is consistent with the intrinsic [6-^{13}C, ^{15}N] KIE obtained experimentally. Color codes for isotopic atoms are the same as described in Figure 4.

Results and Discussion

Synthesis of *ec*TadA Substrate. To determine KIEs of TadA-catalyzed deamination, we prepared the stem loop of *E. coli* tRNA^{arg2} (*ect*RNA^{arg2}) as a minisubstrate and its editing site was isotopically labeled with [1′-^{3}H], [5′-^{3}H$_2$], [1′-^{14}C], [6-^{13}C], [6-^{15}N], [6-^{13}C, 6-^{15}N], and [1-^{15}N] (Figures 1 and S1). The truncated ect*RNA^{arg2} was shown to be as active as full-length ec*tRNA^{arg2} for TadA editing.[1,3,5] Here the KIEs at C6, N6, and N1 positions report on C6 hybridization, extent of N6 dissociation and the degree of N1 protonation at the transition state. The [1′-^{3}H] and [5′-^{3}H$_2$] KIEs are expected to be sensitive to the adenine-ribose glycosyl torsion angle (ring rotation) and any ribosyl distortion between free reactant and the TadA transition state (Figure 4).

Determination of Intrinsic KIEs of TadA-Catalyzed Deamination Reaction. Intrinsic [1′-^{3}H], [5′-^{3}H$_2$], [6-^{13}C], [6-^{15}N], and [1-^{15}N] KIEs were measured for the TadA-catalyzed deamination (Figure 5). V_{max}/K_m ^{3}H KIE experiments were carried out under competitive conditions[18] with the [1′-^{14}C] labeled substrate as the silent competitive isotopic pair (see Experimental Section). Apparent ^{13}C and ^{15}N KIEs were measured using [1′-^{14}C] as the isotopically silent remote label for heavy isotopic substrates (^{13}C or ^{15}N) and [1′-^{3}H] as their

Table 1. Intrinsic KIEs[a] vs Computational KIEs[b] of *ec*TadA

substrate pairs[c]	type of KIEs	intrinsic KIEs vs computational KIEs[d,e]: intrinsic values	computational values
[6-^{13}C, 1′-^{14}C] vs [1′-^{3}H]	α-primary ^{13}C	1.014 ± 0.003	1.014
[6-^{15}N, 1′-^{14}C] vs [1′-^{3}H]	α-primary ^{15}N	1.022 ± 0.002	1.023
[1-^{15}N, 1′-^{14}C] vs [1′-^{3}H]	β-secondary ^{15}N	0.994 ± 0.002	0.994
[6-^{13}C, 6-^{15}N, 1′-^{14}C] vs [1′-^{3}H]	α-primary ^{13}C^{15}N	1.036 ± 0.004	1.037
^{13}C^{15}N calcd[f]	α-primary ^{13}C^{15}N	1.036 ± 0.005	1.037
[1′-^{14}C] vs [5′-^{3}H$_2$]	remote ^{3}H	0.963 ± 0.002	0.966
[1′-^{14}C] vs [1′-^{3}H]	remote ^{3}H	1.014 ± 0.001	1.012

[a] Intrinsic KIEs were obtained upon correcting the remote [1′-^{3}H] KIE for ^{13}k,^{15}k,$^{13,15}k$, and the commitment factor. [b] Computational KIEs were calculated from the frequencies of the substrate and the transition state pairs using ISOEFF98.[30] [6-^{13}C], [6-^{15}N], and [1-^{15}N] KIEs were calculated with 9-methyladenine as a substrate mimic and its hydroxyl adduct as a transition state mimic. 3′-Phosphate-5′-methylphosphate adenosine and its C6 hydroxyl adduct were chosen for [5′-^{3}H$_2$] and [1′-^{3}H] computation. [c] Isotopically labeled positions are indicated. [d] At least 4 measurements were made for each experimental KIE and standard errors are calculated from the variation between experiments. [e] Intrinsic values are from experiencetal KIEs and the "computational values" are the calculated KIE values. [f] Calculated from the product of [6-^{13}C] and [6-^{15}N] KIEs.

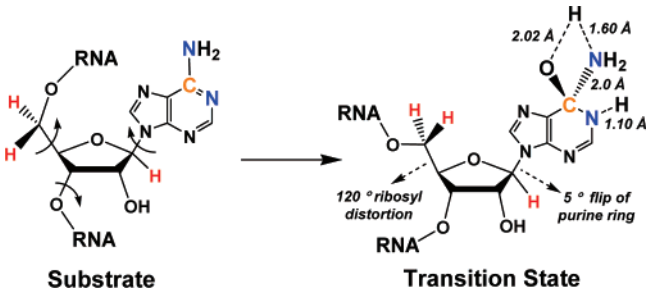

Figure 6. *ec*TadA transition state structure. The *ec*TadA transition state structure was solved using quantum chemical calculations at B3LYP/6-31G(d, p) level of theory (Gaussian98) with the intrinsic KIEs as constraints. [6-^{13}C], [6-^{15}N], and [1-^{15}N] KIEs were adequate to give a unique structure for the deamination chemistry at the transition state. Geometry for the 5′-ribosyl and purine orientation of substrate and the *ec*TadA transition state were selected to match the [5′-^{3}H$_2$]-, and [1′-^{3}H] KIEs and also to be the most similar to the structures of *t*RNA^{Phe} and *t*RNA^{arg2} reported from NMR and X-ray crystallography.[4,23] The interaction distances and dihedral angle variations reflect the altered geometries from free substrate and the *ec*TadA transition state. Color codes for isotopic atoms are the same as described in Figure 4.

competitive isotopic pair. V_{max}/K_m KIEs of [6-^{13}C], [6-^{15}N], and [1-^{15}N] were obtained by correcting the corresponding apparent KIEs with the remote [1′-^{3}H] KIE (Table 1). All KIEs were further subject to correction for forward commitment, which was determined to be $C_f = 0.15$ under an isotope trapping condition (Figure 3). The small value of C_f indicates that the Michaelis complex of TadA converts to product at slower rate than release and equilibration with unbound ectRNA^{arg2} stem loop. Pre-equilibration kinetics are consistent with the modest $k_{cat} = 13$ min^{-1} for this enzyme.[18,19] The intrinsic KIEs of [1′-^{3}H], [5′-^{3}H$_2$], [6-^{13}C], [6-^{15}N], and [1-^{15}N] are 1.014 ± 0.001, 0.963 ± 0.002, 1.014 ± 0.003, 1.022 ± 0.002, and 0.994 ± 0.002, respectively (Figure 5). The accuracy of this set of KIEs was further validated by comparing the [6-^{13}C, ^{15}N] KIE of

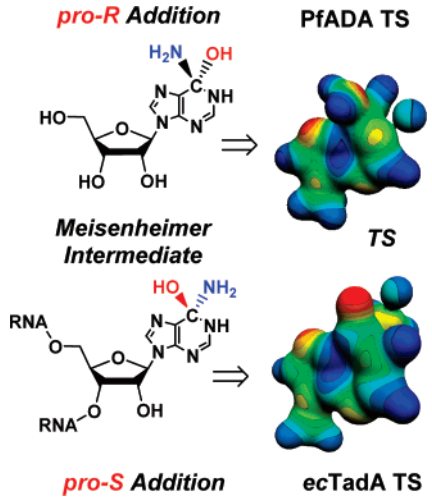

Figure 7. Stereospecific C6 nucleophilic addition. The Zn^{2+}-chelated hydroxyl of *ec*TadA attacks the substrate C6 center from the *pro-S* face in contrast to the stereospecific *pro-R* hydroxyl addition for *Plasmodium falciparum*, human and bovine adenosine deaminases.[18] Left, Meisenheimer intermediates; right, MEP of transition states (9-methyladenine mimics used here).

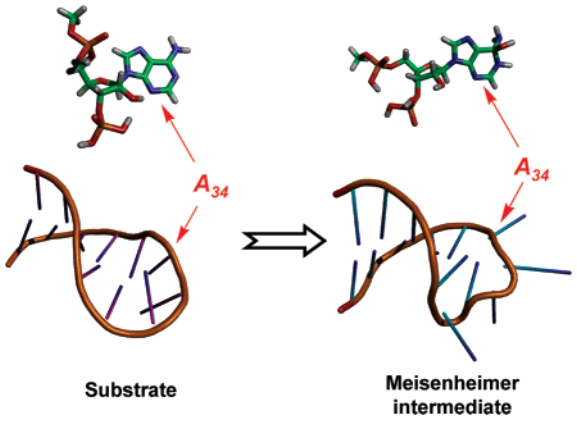

Figure 8. Base rotation at the *ec*TadA transition state. 5′-Ribosyl distortion and purine ring rotation occur on the path to formation of the *ec*TadA Meisenheimer intermediate and the transition state. (Top) Comparison of unbound substrate and Meisenheimer intermediate A_{34} conformations (C, green; H, gray; O, red; N, blue; P, brown). (Bottom) Cartoon for the base rotation process. The two cartoon structures represent the stem loop regions of *ec*tRNA^{Phe} (PDB, 1KKA)[23] and TadA-bound RNA^{arg2} (PDB, 2B3J),[4] respectively. The structures were directly generated from the corresponding PDB files.

1.036 ± 0.004, in good agreement with the product of the corresponding primary [6-^{13}C] and [6-^{15}N] KIEs (Figure 5).

Computational Modeling of *ec*TadA Transition State Structure. We applied the intrinsic KIEs as constraints to match *ec*TadA transition state structures modeled by Gaussian98 at the B3LYP/6-31G(d,p) level (see the Experimental Section). To compute *ec*TadA transition state structures, 9-methyladenine was used as a reactant mimic and a hydroxyl anion was used as the nucelophile.[18] Upon systematically varying C6-O^{hydroxyl}, C6−N6 bond distances as well as the degree of O^{hydroxyl}, N1, and NH$_2$-6 protonation, a single transition state structure was found to match the intrinsic [6-^{13}C], [6-^{15}N], and [1-^{15}N] KIEs of *ec*TadA (Table 1, Supporting Information) and therefore represents the best estimate of transition state structure for the TadA-catalyzed deamination (Figure 6). In contrast to the early S_NAr character of nucleotide adenosine deaminase (ADA),[18] *ec*TadA adopts a late S_NAr transition state with a complete, *pro-*

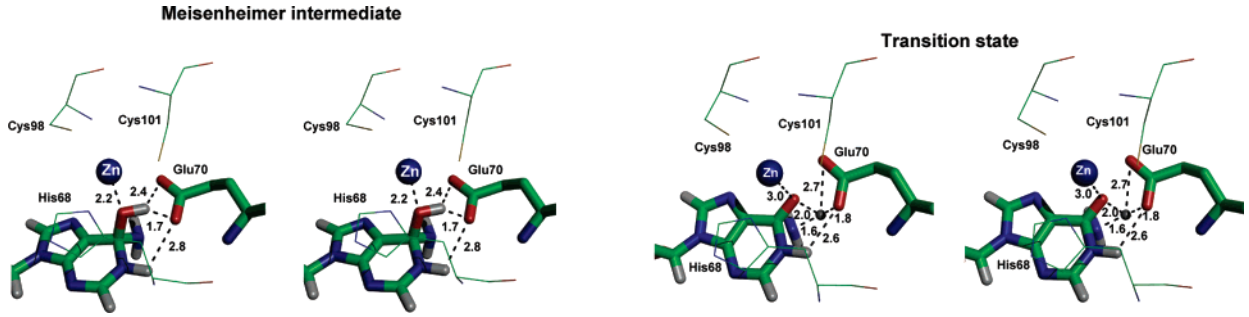

Figure 9. Steric view of docking structures of the Meisenheimer intermediate (left) and the transition state (right) at enzyme active site. Lines, His68, Cys98, and Cys101; sticks, Glu70, intermediate, and transition state; green, carbons; blue, nitrogens; red, oxygens; yellow, sulfurs; blue sphere, Zn; gray sphere, the shuttled proton; dashed line, key interaction distances for enzyme catalysis labeled in angstroms. The structures were generated by docking the solved structures of the *ec*TadA Meisenheimer intermediate and transition state structure into the enzyme active site (PDB, 1Z3A). *ec*TadA was first aligned with *S. aureus* TadA (PDB, 2B3J) and then the nebularine ribosyl moiety was used as a guide to overlay with the ribosyl moieties of the *ec*TadA Meisenheimer intermediate and the transition state. PyMOL (W. L. DeLano, PyMOL Molecular Graphics System) was used for illustration.

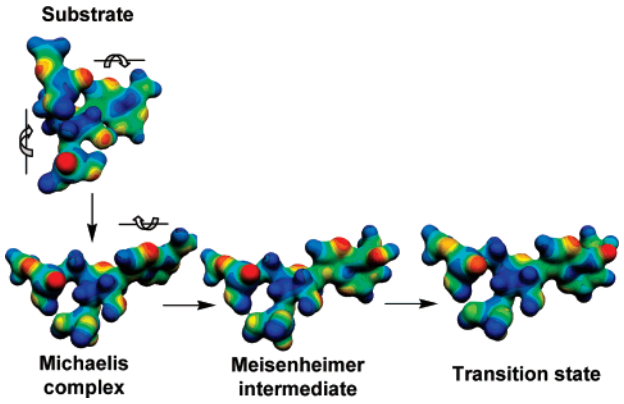

Figure 10. Molecular electrostatic potential (MEP) surfaces of stepwise structures. MEP surfaces of substrate, Michaelis complex, Meisenheimer intermediate, and the *ec*TadA transition state were generated using the CUBE subprogram of Gaussian 98 and visualized using Molekel 4.0 at a density of 0.15 electron/Å^3. The [5′-$^3H_2$] and [1′-^{3}H] KIEs are proposed to be generated as the reaction processes from the unbound substrate to the *ec*TadA-stabilized Michealis complex.

S-face hydroxyl attack and nearly complete N1 protonation (Figure 7). The N1 protonation at the transition state is consistent with a [1-^{15}N] KIE of 0.994 and a N1−H distance of 1.10 Å. A fully protonated N1 at the transition state corresponds to a [1-^{15}N] KIE of 0.989 and an N1-H distance of 1.05 Å. Significant N6−C6 dissociation at the *ec*TadA transition state is reported by the large [6-^{15}N] KIE of 1.022 and corresponds to a N6−C6 distance of 2.0 Å at the transition state. A unique feature of the transition state is the partial proton transfer from the attacking hydroxyl nucleophile to the 6-NH_2 leaving group with a H−O distance of 2.02 Å and a H−N distance of 1.60 Å, respectively.

Remote [5′-$^3H_2$] KIEs. The remote [5′-$^3H_2$] KIE is a remarkable inverse −3.7% (0.963 ± 0.002) for *ec*TadA (Figure 5). This large remote KIE arises as a consequence of 5′-ribosyl distortion at the *ec*TadA editing site on the path to forming the transition state. We propose that this 5′-ribosyl distortion occurs prior to the *pro-S-face* hydroxyl attack because the purine base rotation into TadA active site is a prerequisite step for the subsequent editing (see discussion below) and KIEs report all the steps between free reactants and the first chemically irreversible step, in this case, the hydrolytic deamination following transition state formation. The 5′-tritium of the reactive adenosine is eight bonds from TadA reaction center and is not expected to be sensitive to deamination at the C6 position.[18,19] However, remote ^{3}H substitution can be influenced by local geometrical distortion at enzyme-bound transition states.[19,24]

The 5′-ribosyl distortion at the *ec*TadA transition state was explored by computational chemistry for altered 5′-geometries that generate the 0.963 inverse [5′-$^3H_2$] KIE. Pairs of substrate and transition state candidates for [5′-$^3H_2$] computation were generated by altering the [5′-$^3H_2$] KIE-sensitive dihedral angles at the corresponding *ec*TadA-editing site on the basis of *t*RNA structures (see the Experimental Section).[4,23] The structures that match the experimental KIE show a characteristic O5−C5′−C4′−O4 dihedral angle of −68° for unbound substrate and of 172° for the TadA-bound transition state. This variation corresponds to a 120° rotation of the adenosine-A_{34} 5′-hydroxyl moiety at the transition state relative to the unbound substrate (Figure 8). Therefore, *ec*TadA binding to RNA induces a conformational change at the stem loop region of the substrate. This interaction is essential for *ec*TadA-mediated A-to-I editing because it makes the A_{34} residue, in particular its purine ring, fully exposed and thus provides ready access into the enzyme active site (Figure 8−10). For the 5′-ribosyl group, the KIE-derived geometries of the substrate and *ec*TadA transition state are similar to but not the same as in structures of unbound *t*RNA^{Phe} and TadA-bound *t*RNA^{arg2} analogue, which have been solved by NMR and X-ray crystallography, respectively (Supporting Information).[4,23] The structural difference stems from varied dihedral angles (less than 20 degrees) around the A_{34} 5′-ribosyl region and are within the resolution limitation of NMR and X-ray structures (Supporting Information).

Remote [1′-^{3}H] KIEs. The *ec*TadA-mediated deamination reaction also displays an unexpected but significant [1′-^{3}H] KIE of 1.4%. This remote KIE can arise from the C1′-N9 bond rotation.[19] Every 1−2% KIE corresponds to 10° rotation of the purine ring from its geometry in free reactant to enzyme-bound transition state.[19] We interpreted the 1.4% [1′-^{3}H] KIE as a signal of the purine rotation around the ribosidic bond that occurs prior to the *pro-S-face* hydroxyl attack (the same argument as for [5′-$^3H_2$] KIE above). Computational modeling results indicated that alteration of the C8−N9−C1′−O4 dihedral angle from 39° for unbound substrate to 45° at the transition state accounts for the observed [1′-^{3}H] KIE (Figure 8−10). As demonstrated by the docking models (Figure 9 and results below), this C1′−N9 purine rotation places the Zn-bound

(24) Birck, M. R.; Schramm, V. L. *J. Am. Chem. Soc.* **2004**, *126*, 6882−6883.

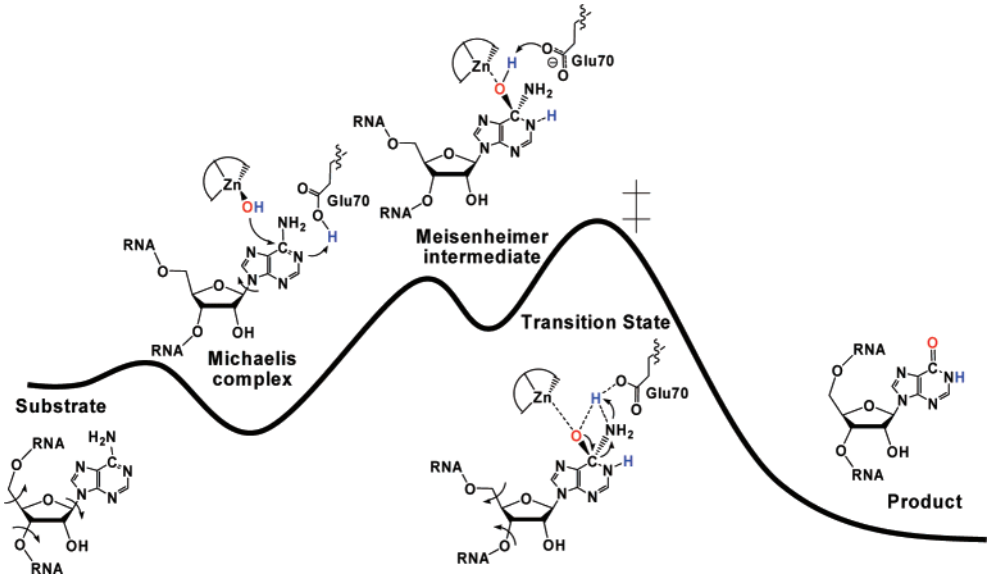

Figure 11. Stepwise mechanism proposed for the *ec*TadA-mediated A-to-I editing. The transition state is the highest energetic barrier along the reaction coordinate. The overall energy profile is relative and the corresponding structures are displayed with the arrows for bond rotation or electron flow in each step. The Zn^{2+}-chelated hydroxyl and the proton of the catalytically essential Glu70 are highlighted.

hydroxyl adjacent to C6 of the edited A_{34} residue and therefore facilitates the subsequent hydroxyl nucleophilic addition. The KIE-derived C8−N9−C1′−O4 dihedral angle at the *ec*TadA transition state (computed to be 45°) is around 30° smaller than found for the chemically unreactive complex of the TadA-bound *t*RNA^{arg2} analogue (73°).[4] The TadA-bound *t*RNA^{arg2} analogue has been proposed to mimic the enzyme-bound substrate (Michaelis complex).[4] However, variation of the C8−N9−C1′−O4 dihedral angles from 39 to 45° are sufficient to explain adenine exposure and the transition state geometry for *ec*TadA (Figure 10).

Docking the Transition State Structure Into the Active Site of *ec*TadA. Crystal structures of bacterial TadAs reveal RNA structural motifs in relation to the Zn^{2+} binding pocket for the deamination reaction.[1−4] Models of the *ec*TadA Meisenheimer intermediate and the transition state structure were docked into the active site of substrate-analogue-bound *Staphylococcus aureus* TadA to explore the architecture for *ec*TadA catalysis (Figure 9). The docking model shows that *ec*TadA Glu70 is within hydrogen bond distances to N1, N6 and O^{hydroxyl} in the docking models (Figure 9). Consequently, the Glu70 residue can interact with both the N1 amide proton and serve as a proton shuttle between the N6-O^{hydroxyl}. Docking models with the transition state support the process. The possibility that N6 proton was transferred from nearby water rather than the O^{hydroxyl} was ruled out because the *pro-S-face* hydroxyl attack makes N6 buried into a solvent-exclusive pocket (docking structure not shown). The interaction between *ec*TadA Glu70 and the N1 amide bond also supports its function as a proton donor for the formation of N1 amide bond at the step of Zn^{2+}-activated hydroxyl nucleophilic addition (discussion below and Figure 11).

The catalytically essential zinc ion coordinates the O^{hydroxyl} with distances of 2.2 Å and 3.0 Å in the *ec*TadA Meisenheimer intermediate and transition state models, respectively. The Zn^{2+}-chelated O6^{hydroxyl} of the Meisenheimer intermediate is positioned for a reversible nucleophilic attack at C6 of the adenine. In contrast, the Zn^{2+}-O^{hydroxyl} bond has weakened an additional 0.8 Å at the *ec*TadA transition state. The 5′-ribosyl distortion and C1′-N9 ribosidic purine rotation (results above) also contribute to the position of the Zn^{2+}-hydroxyl. In the Meisenheimer complex the O6^{hydroxyl} is shifted by 40° away from the Zn^{2+}-coordinated water in the *ec*TadA crystal structure, reflecting reorientation of the hydroxyl nucelophile to form the intermediate.

Stepwise Reaction Mechanism of *ec*TadA-Catalyzed Deamination Reaction. A stepwise reaction mechanism for *ec*TadA is based on the structures of the TadA-bound substrate analogue and the *ec*TadA transition state structure reported here (Figure 10, 11). Formation of the Michaelis complex is accompanied by a 120° distortion at the A_{34} 5′-region of the RNA and generates an inverse 4% [5′-$^3H_2$] KIE. The purine rotates 34° based on the C8−N9−C1′−O4 dihedral of 39° for the unbound substrate relative to 73° in the Michaelis complex. The *ec*TadA-*ect*RNA^{arg2} Michaelis complex shows an additional 28° purine rotation (C8−N9−C1′−O4 dihedral angle = 45°). Meanwhile, attack of the Zn^{2+}-chelated water at C6 of A_{34} is accompanied by Glu70-mediated N1 protonation, to form the tetrahedral Meisenheimer intermediate. These steps generate a [1′-^{3}H] KIE of 1.014 and a [1-^{15}N] KIE of 0.994. The highest chemical barrier on the reaction coordinate defines the transition state and involves the Glu70-facilitated proton shuttle from the O^{hydroxyl} to N6, reflected by [6-^{13}C] and [6-^{15}N] KIEs of 1.014 and 1.022, respectively. This is followed by N6 dissociation in a step after the transition state formation.

Comparison of the Transition State Structures of *ec*TadA and Other Deaminases. Two features distinguish the transition state structure of *ec*TadA from those of adenosine deaminases (ADA) but relate the *ec*TadA to cytidine deaminase (CDA). First, both CDA and *ec*TadA adopt late S_NAr transition states following the formation of the Meisenheimer intermediate.[25] This transition state is characterized by complete hydroxyl-C6 bond formation, nearly complete N1 protonation, and partial N6 amino group dissociation. In contrast, the transition states

(25) Snider, M. J.; Reinhardt, L.; Wolfenden, R.; Cleland, W. W. *Biochemistry* **2002**, *41*, 415−421.

of ADAs show significant early S_NAr character with incomplete N1 protonation and no C6−N6 dissociation.[18] More remarkably, the Zn^{2+}-hydroxyls of *ec*TadA and CDA approach their targeted bases from the *pro-S*-face in contrast to the *pro-R*-face attack for ADAs (Figure 7). The stereospecific hydrolysis of these enzymes is consistent with the structures of enzyme-bound nonhydrolyzable substrate analogues[2,26,27] and stereospecific transition-state analogue inhibitors.[18,28,29] In spite of chemistry most similar to adenylate deamination reactions, the distinct late S_NAr transition state and stereospecificity of TadA argue that this enzyme is mechanistically more related to CDA rather than to ADAs.

Conclusion. The A-to-I RNA editing enzymes have received attention due to their complex RNA substrates and still-evolving biological functions. Here, we applied KIEs and quantum molecular modeling to solve the transition state structure of *ec*TadA. Together with docking studies, the work supports a stepwise mechanism for the *t*RNA editing process. The key events are facilitated by the enzyme-promoted base flip and the Glu70-mediated proton shuttle. Given the sequence similarity at the catalytic domains of TadA and ADAR families, it is likely that similar transition state structures have been adopted by the ADARs. The structural features of this transition state, such as the *S*-face hydroxyl, the amino group dissociation and the interaction between the shuttled proton and the nearby Glu residue, are informative for the development of tight-binding inhibitors.

Acknowledgment. We thank J. Kim and S. C. Almo (Albert Einstein College of Medicine) for the *ec*TadA plasmid and J. Gao of the University of Minnesota Supercomputer Institute for computer time. This work was supported by NIH grant CA72444.

Supporting Information Available: Detailed methods, Figure S1, and structures of optimized substrates, intermediates and transitions. See Supporting Information online. This material is available free of charge via the Internet at http://pubs.acs.org.

JA078008X

(26) Ireton, G. C.; Black, M. E.; Stoddard, B. L. *Structure* **2003**, *11*, 961−972.
(27) Sharff, A. J.; Wilson, D. K.; Chang, Z.; Quiocho, F. A. *J. Mol. Biol.* **1992**, *226*, 917−921.
(28) Tyler, P. C.; Taylor, E. A.; Frohlich, R. F.; Schramm, V. L. *J. Am. Chem. Soc.* **2007**, *129*, 6872−6879.
(29) Chung, S. J.; Fromme, J. C.; Verdine, G. L. *J. Med. Chem.* **2005**, *48*, 658−660.
(30) Anisimov, V.; Paneth, P. *J. Math. Chem.* **1999**, *26*, 75−86.